A NEW GENERATION OF ANTENNA STRUCTURES BASED ON NOVEL COMPOSITE MATERIALS

ARO FINAL REPORT

AUGUST 1, 1998 - JANUARY 1, 1999
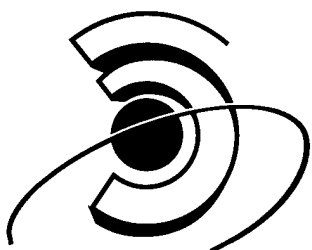
GRANT # DAAG55-98-1-0412

Contract #037348

INVESTIGATORS:

LINDA P.B. KATEHI
KAMAL SARABANDI

UNIVERSITY OF MICHIGAN
RADIATION LAB
1301 BEAL AVENUE
3240 EECS BUILDING
ANN ARBOR, MICHIGAN 48109-2122

Radiation Laboratory
Department of Electrical Engineering
and Computer Science
Ann Arbor, Michigan 48109-2122
USA

19991215 047

THE UNIVERSITY OF MICHIGAN

REPORT DOCUMENTATION PAGE

Form Approved
OMB NO. 0704-0188

Public Reporting burden for this collection of information is estimated to average 1 hour per response, including the time for reviewing instructions, searching existing data sources, gathering and maintaining the data needed, and completing and reviewing the collection of information. Send comment regarding this burden estimates or any other aspect of this collection of information, including suggestions for reducing this burden, to Washington Headquarters Services, Directorate for information Operations and Reports, 1215 Jefferson Davis Highway, Suite 1204, Arlington, VA 22202-4302, and to the Office of Management and Budget, Paperwork Reduction Project (0704-0188,) Washington, DC 20503.

1. AGENCY USE ONLY (Leave Blank)	2. REPORT DATE - November 22, 1999	3. REPORT TYPE AND DATES COVERED 01 August 1998 - 31 May 1999

4. TITLE AND SUBTITLE A New Generation of Antenna Structures Based on Novel Composite Materials	5. FUNDING NUMBERS DAAG55-98-1-0412
6. AUTHOR(S) Linda P.B. Katehi and Kamal Sarabandi	

7. PERFORMING ORGANIZATION NAME(S) AND ADDRESS(ES) University of Michigan Ann Arbor, MI 48109-2122	8. PERFORMING ORGANIZATION REPORT NUMBER

9. SPONSORING / MONITORING AGENCY NAME(S) AND ADDRESS(ES) U. S. Army Research Office P.O. Box 12211 Research Triangle Park, NC 27709-2211	10. SPONSORING / MONITORING AGENCY REPORT NUMBER ARO 37353.1-EL-II

11. SUPPLEMENTARY NOTES
    The views, opinions and/or findings contained in this report are those of the author(s) and should not be construed as an official Department of the Army position, policy or decision, unless so designated by other documentation.

12 a. DISTRIBUTION / AVAILABILITY STATEMENT Approved for public release; distribution unlimited.	12 b. DISTRIBUTION CODE

13. ABSTRACT (Maximum 200 words)

Antenna miniaturization is always desirable as the communication apparatus becomes more and sophisticated and the physical space becomes an expensive commodity. It is possible to reduce the size of the antenna by altering its shape and the properties of the material it is made of. In this study, we load a slot ring radiator with a finite dielectric lens, which increases the propagation constant around the antenna as well as over its aperture and therefore relaxes the size requirement. The amount of miniaturization depends both on the electromagnetic properties as well as the volume of the lens. The regular practice is to choose a pure dielectric and employ a high permittivity. However,

(CONTINUED ON NEXT PAGE)

14. SUBJECT TERMS	15. NUMBER OF PAGES 7
	16. PRICE CODE

17. SECURITY CLASSIFICATION OR REPORT UNCLASSIFIED	18. SECURITY CLASSIFICATION ON THIS PAGE UNCLASSIFIED	19. SECURITY CLASSIFICATION OF ABSTRACT UNCLASSIFIED	20. LIMITATION OF ABSTRACT UL

NSN 7540-01-280-5500

Standard Form 298 (Rev.2-89)
Prescribed by ANSI Std. 239-18
298-102

controlling the loss becomes a major issue at high dielectric constants. Or one may choose to use a larger or thicker lens together with a lower permittivity. We chose to study a lens with electrical as well as magnetic properties (relative permeability is larger than unity), because the effective propagation constant is proportional to the product of the effective permittivity and permeability ($\sqrt{\mu_r \varepsilon_r}$), the use of magnetic materials will relax the requirement on high values of permittivity for a small size of the lens antenna.

A NEW GENERATION OF ANTENNA STRUCTURES BASED ON NOVEL COMPOSITE MATERIALS

Abstract

Antenna miniaturization is always desirable as the communication apparatus becomes more and sophisticated and the physical space becomes an expensive commodity. It is possible to reduce the size of the antenna by altering its shape and the properties of the material it is made of. In this study, we load a slot ring radiator with a finite dielectric lens, which increases the propagation constant around the antenna as well as over its aperture and therefore relaxes the size requirement. The amount of miniaturization depends both on the electromagnetic properties as well as the volume of the lens. The regular practice is to choose a pure dielectric and employ a high permittivity. However, controlling the loss becomes a major issue at high dielectric constants. Or one may choose to use a larger or thicker lens together with a lower permittivity. We chose to study a lens with electrical as well as magnetic properties (relative permeability is larger than unity), because the effective propagation constant is proportional to the product of the effective permittivity and permeability ($\sqrt{\mu_r \varepsilon_r}$), the use of magnetic materials will relax the requirement on high values of permittivity for a small size of the lens antenna.

Numerical Simulationss,

The antenna analyzed is shown in Figure 1(a). A slot ring radiator is printed on an infinite ground plane and is loaded with a finite thick dielectric lens. The outer diameter of the ring is 3cm and the slot is 0.2cm wide. The lens is 1.5cm thick with a 6cm diameter, and its permittivity and permeability are allowed to vary.

The finite element method (FEM) has been used for the computation of the near field for an ideal current source excitation extended across the slot as shown in Figure 1(b). A finite volume around the ring+lens combination is designated as the solution space, which is discretized using finite volumes, each with linear dimensions on the order of $\lambda/20$. First the 2-D mesh is created using triangles and quadrilaterals across the ring and the lens surface. Volume mesh is created by repeating the same surface mesh over successive vertical layers, each of which is again approximately $\lambda/20$. The resulting volume elements are right prisms with triangular and quadrilateral cross-sections. The solution space is terminated using a metal-backed absorber (a lossy dielectric layer). Average problem size was 33,000 unknowns, consuming 56MB of memory and requiring 30-100 minutes of CPU time for one frequency point.

Miniaturization study

1. Through permittivity and permeability

The simulation showed that for most of the values of the ε - µ pair, there were two resonances. The primary and secondary resonances are shown in Figure 3(a) as a function of ε and µ values in blue and red color, respectively. Note that the second resonance data are missing for the cases when the resonance did not exist or was not visible enough to characterize it as such. Also given is the theoretical value for the resonance frequency of an infinite lens (*black*), which has the same permittivity and permeability as the finite lens under examination. This value is based on the effective quantities (see Figure 3b) and is given by

$$f_o = \frac{f_{air}}{\sqrt{\varepsilon_{eff}\mu_{eff}}}$$

where f_{air} = 3.8065GHz, the resonance frequency of the ring in the absence of a lens. The secondary resonances become more visible as the refractive index of the lens increases. This leads us to believe that the secondary resonances are most probably caused by the standing waves inside the lens, i.e., due to the finite size of the lens.

Figure 4 shows the variation of the fractional bandwidth in the ε–µ plane for both the primary and the secondary resonances. Note that the bandwidth data are again not provided for cases, where the resonance did not exist, or the resonance did not resemble a parallel RLC circuit behavior (i.e., imaginary part vanishes right after real part peaks) or the bandwidth was too small to quantify.

2. Through lens size increase

As the dielectric constant of the material increase so do the losses and it is an expensive process to control losses. Fortunately, when the highest permittivity or the permeability one can manufacture is limited, the rest of the miniaturization can be made up for by using a thicker or larger lens. Table 1 shows three different sizes of lens and the resulting resonance frequencies as the permittivity and permeability are changed but kept equal. The fist column is the same antenna as the one analyzed above, i.e., it shows the data along the diagonal of the 2-D plot in Figure 3(a). The other two columns are for larger lens size and slot width.

3
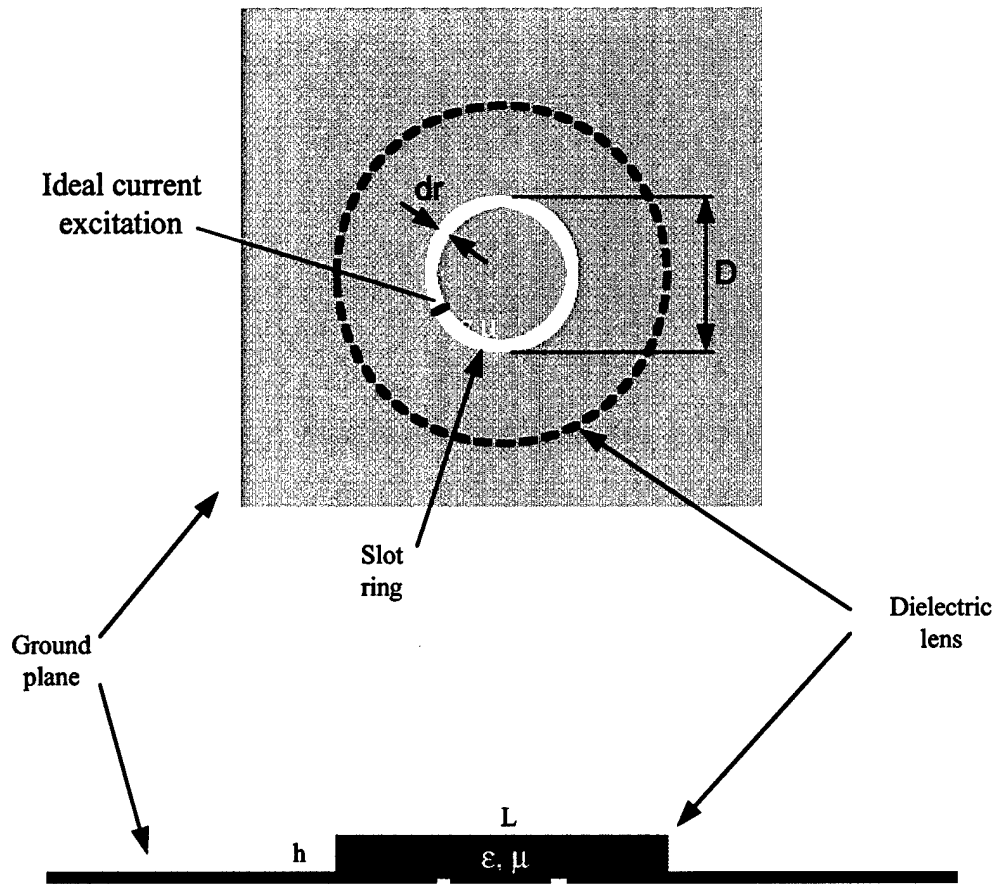
Figure 1: Geometry of the slot-ring radiator loaded with a finite magnetic dielectric lens. h=1.5cm, L = 6cm, D=3cm, dr=0.2cm.
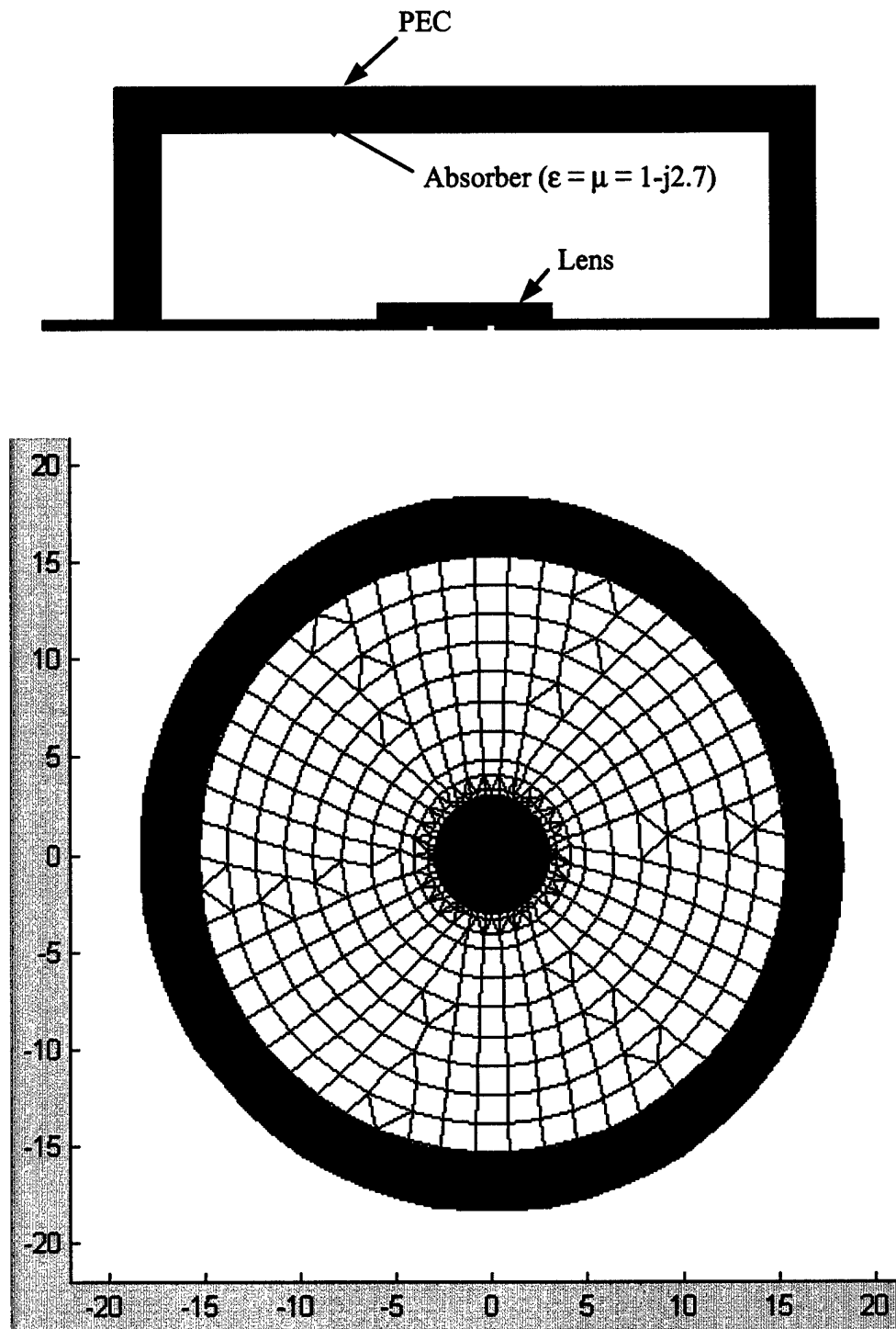
Figure 2: Finite element modeling of the ring+lens combination. Surface mesh composed of triangles and quadrilaterals and the metal-backed absorber layer (lossy dielectric) used to terminate the solution space are shown.
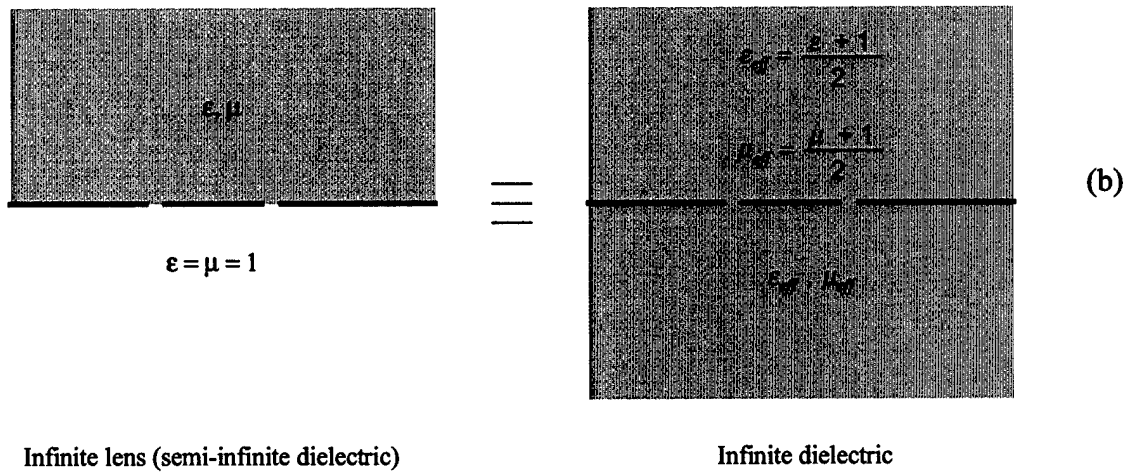
Resonance Frequency (GHz), Blue:first, Red:second, Black: Infinite lens

Relative permittivity (y-axis) vs Relative permeability (x-axis)

At permittivity ≈ 15:
- 1.1529 / 0.9585 / 0.766 / 0.6705
- 0.7896 / 0.6791 / 0.5539
- 1.3458 / 0.777 / 0.57385 / 0.47581

At permittivity ≈ 10:
- 1.3947 / 1.1571 / 0.9367 / 0.8133
- 0.9582 / 0.7992 / 0.6539
- 1.6231 / 0.9371 / 0.69209 / 0.57385

At permittivity ≈ 5:
- 1.9186 / 1.5696 / 1.284 / 1.1278
- 1.05 / 0.8378
- 2.1977 / 1.2688 / 0.9371 / 0.777

At permittivity ≈ 1:
- 3.8065 / 2.7949 / 2.5282 / 2.4155
- 1.3875
- 3.8065 / 2.1977 / 1.6231 / 1.3458

(a)

ε, μ

$\varepsilon = \mu = 1$

$\varepsilon_{eff} = \dfrac{\varepsilon + 1}{2}$

$\mu_{eff} = \dfrac{\mu + 1}{2}$

$\varepsilon_{eff}, \mu_{eff}$

(b)

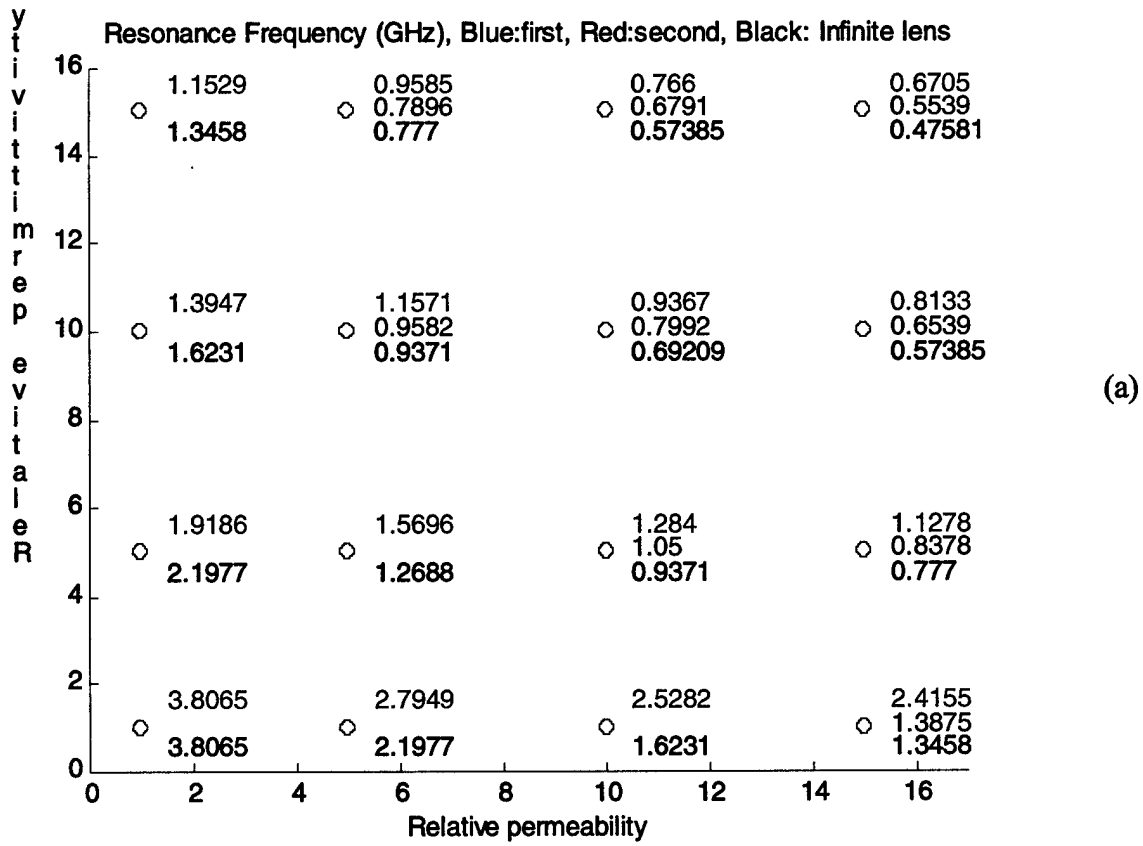Infinite lens (semi-infinite dielectric)   Infinite dielectric

Figure 3: (a) Variation of the primary (blue) and secondary (red) resonances in the
μ–ε (permeability-permittivity) plane including the theoretical value for infinite lens
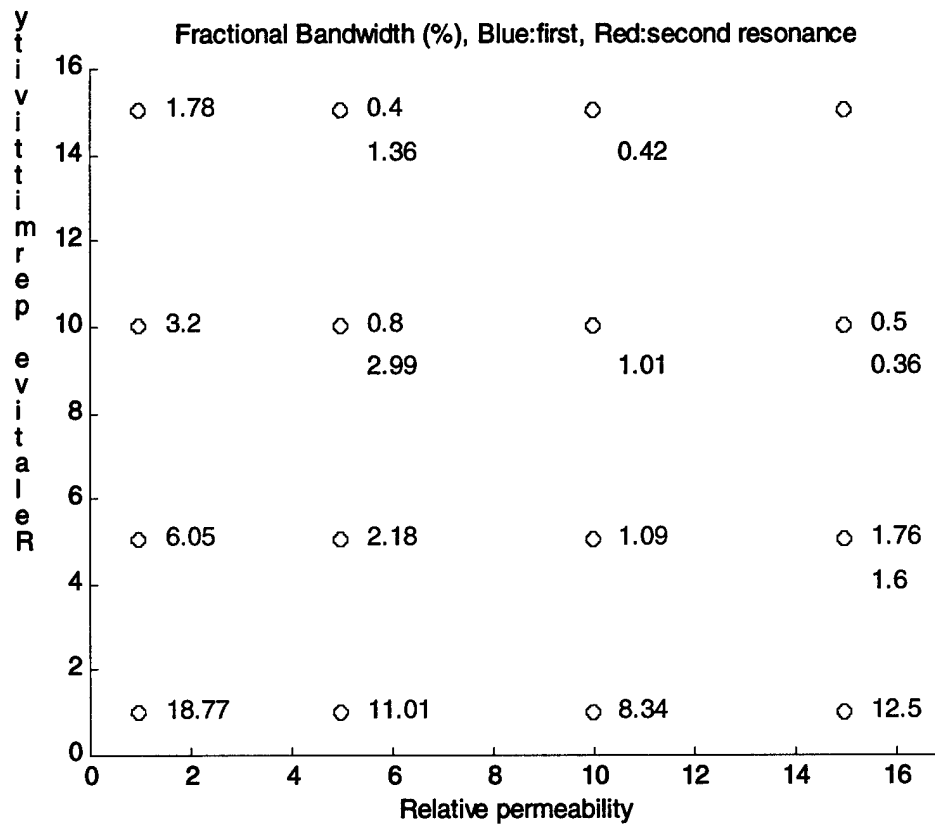(black), (b) explanation of the ε_{eff} and μ_{eff}.

6

Fractional Bandwidth (%), Blue:first, Red:second resonance

Relative permittivity (y-axis) vs Relative permeability (x-axis)

Data points (Blue: first resonance / Red: second resonance):

- Permittivity 15: (μ≈1) 1.78; (μ≈5) 0.4 / 1.36; (μ≈10) — / 0.42; (μ≈15) —
- Permittivity 10: (μ≈1) 3.2; (μ≈5) 0.8 / 2.99; (μ≈10) — / 1.01; (μ≈15) 0.5 / 0.36
- Permittivity 5: (μ≈1) 6.05; (μ≈5) 2.18; (μ≈10) 1.09; (μ≈15) 1.76 / 1.6
- Permittivity 1: (μ≈1) 18.77; (μ≈5) 11.01; (μ≈10) 8.34; (μ≈15) 12.5

Figure 4: Variation of the fractional bandwidth for the primary (blue) and secondary (red) resonances in the μ–ε (permeability-permittivity) plane.

$\varepsilon = \mu$	fo (MHz)	$\varepsilon = \mu$	fo (MHz)	$\varepsilon = \mu$	fo (MHz)
1	3807	1		1	
5	1572	5		5	
10	957	10		10	
15	700	15	260	15	210
25		25	180	25	
50		50	140	50	

L = 6 cm	L = 18 cm	D = 18 cm
h = 1.5cm	h = 2.25cm	h = 5cm
D = 3cm	D = 9cm	D = 9cm
dr = 0.2cm	dr = 0.6cm	dr = 0.6cm

Table 1: Resonance frequencies for different $\mu = \varepsilon$ values for three different lens sizes.